Monte Carlo Simulation of Flux Lattice Melting in a Model High-T_c Superconductor

S. Ryu,[1] S. Doniach,[1] Guy Deutscher,[2] and A. Kapitulnik[1]
[1]*Department of Applied Physics, Stanford University, Stanford, California 94305*
[2]*School of Physics and Astronomy, Tel-Aviv University, Ramat-Aviv, 69978, Israel*
(Received 24 July 1991)

We studied flux lattice melting in a model high-T_c superconductor by Monte Carlo simulation in terms of vortex variables. We identify two melting curves in the B-T phase diagram and evaluate a density-dependent Lindemann criterion number for melting. We also observe that the transition temperature shifts downward toward the two-dimensional melting limit as the density of flux lines increases. Although the transition temperature does not change, a significant difference in shear modulus is observed when flux cutting or reconnection is allowed.

PACS numbers: 74.60.Ge, 02.50.+s

In the high-temperature superconductors (HTSC), due to strong anisotropy and the high transition temperature, thermal fluctuations of the vortices induced by an applied magnetic field are believed to play an important role in most of the H-T plane [1]. The cuprates are all strongly type-II materials ($\kappa \cong 100$) with high anisotropy (effective-mass ratio as large as 100) and very short coherence lengths [typically $\xi_{ab}(0) \simeq 10$ Å]. Thus, instead of forming a rigid Abrikosov lattice, each flux line is expected to have considerable lateral fluctuations normal to the direction of applied magnetic field. The possibility of the melting of the flux lattice in two-dimensional superconducting thin films was first pointed out by Huberman and Doniach [2] and later by Fisher [3] based on the dislocation-mediated melting theory [4]. Melting of the 3D flux lattice in HTSC belongs to a different universality class and it may show a crossover from the 3D behavior to the quasi-2D behavior as one varies the areal density of the system.

Because of the complexities of the problem, it is highly desirable to study a simple yet plausible model system through both experiments [5] and computer simulations to shed light on the essentials of the problem. Among the issues yet to be fully understood are the relevance of the melted flux liquid [1] and the vortex glass [6,7], the importance of flux cutting and reconnection [8] in the context of the disentangled and entangled liquid regimes, and effects of the "quasi-two-dimensionality" and the weak interlayer coupling on the melting transition [9]. All of these may be effectively studied in a well-controlled simulation. Recently, Xing and Tešanović [10] did a variational Monte Carlo (MC) simulation of the analogous boson system and observed a melting transition for the Y-Ba-Cu-O system very close to the H_{c1} line, while Li and Teitel [11] studied the anisotropic frustrated 3D XY model and analyzed the helicity moduli and some effects of the vortex cutting. In this Letter, we present the first MC simulation of the flux-line system over a wide range of the phase diagram with a realistic interaction which can be directly related to real materials. We show results that address most of the questions raised above.

A reasonable starting point is to take the Lawrence-Doniach (LD) model of stacked superconducting layers [12] with a free energy given by

$$\mathcal{F}_{\mathrm{LD}}=\frac{aH_c^2(0)}{8\pi}\sum_z\int d^2\rho\left\{|\xi_{ab}(T)(\nabla_{ab}-i2e\mathbf{A}_{ab})\psi_z|^2+\left(1-\frac{T}{T_c}\right)|\psi_z|^2+\tfrac{1}{2}\beta|\psi_z|^4 -g\left|\exp\left(2ie\int_{z_{n+1}}^{z_n}dz\cdot\mathbf{A}_z\right)\psi_{z+1}-\psi_z\right|^2\right\}+\frac{1}{8\pi}\int d^3x\,\mathbf{B}^2(r)\,. \tag{1}$$

In a fixed external field $\mathbf{H}_{\mathrm{ext}}$ one needs to consider the Gibbs free energy $\mathcal{G}_{\mathrm{LD}}=\mathcal{F}_{\mathrm{LD}}-(1/4\pi)\int d^3x\,\mathbf{B}\cdot\mathbf{H}_{\mathrm{ext}}$. We consider a stack of superconducting layers each of thickness d, interlayer spacing a, and dimensionless interlayer coupling strength g. From now on, we concentrate on the case where the field is applied perpendicular to the planes. We model the thermodynamics of Eq. (1) in terms of a vortex representation. The position vector of a segment of the ith vortex line in the zth plane is denoted by $R_{i,z}$. The mean distance between neighboring vortices is a_0. A pair of segments of a single flux line interact with each other via the magnetic interaction ($\int d^3r\,\mathbf{j}\cdot\mathbf{A}$) and the Josephson coupling (the "g-coupling term") between successive layers. They are both quadratic for a small separation of vortices in adjacent layers ($|R_{i,z}-R_{i,z+1}| \ll \lambda$). The Josephson coupling can be shown to be larger than the other by a factor $\sim g\kappa^2(a/d)^2 \sim 10$ for $Bi_2Sr_2Ca_1Cu_2O_8$ [13]. For large separation, the magnetic coupling grows logarithmically and is again negligible compared to the linear effect of the Josephson coupling [14]. It can also be shown that the interaction of a flux line with the external field can be neglected [15]. The Josephson coupling leads to the interaction of a pair of displaced segments,

$$\delta F_J^{z,z+1}=\frac{\Phi_0^2 g}{16\pi^3\lambda^2 a}\int d^2\rho[1-\cos(\phi_z-\phi_{z+1})]\,, \tag{2}$$

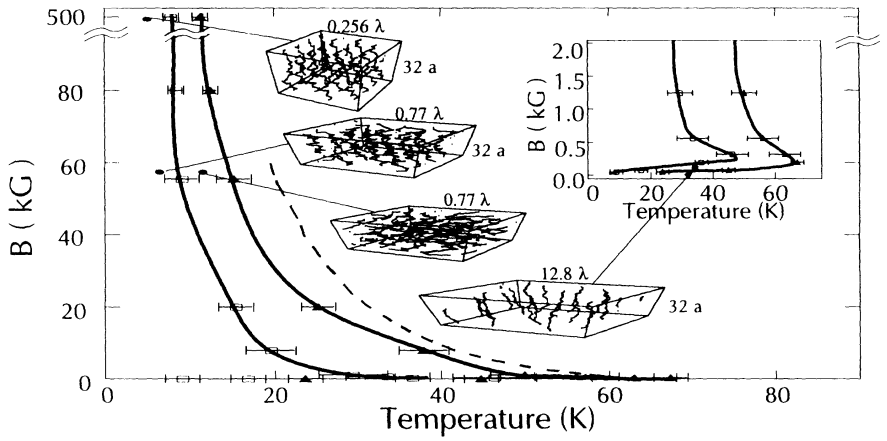

FIG. 1. B vs T phase diagram for $B=12.5$ G to 50 T. Two curves from the simulations are shown. The lower-temperature curve (open squares) represents the points where the translational order parameter drops to zero. The other curve (solid triangles) is for the bond-angle order parameter. The results from elastic continuum theory [22] are also shown (dashed line) for comparison. Some typical configurations are displayed. Note that each box carries its size in units of λ and a, the interlayer spacing. The apparent aspect ratio is not exact. Inset: The very-low-density region.

where ϕ_z is the phase of the condensate order parameter at zth plane. For $|R_{i,z}-R_{i,z+1}|$ much smaller than a length scale defined by $r_g \equiv \xi_{ab}/\sqrt{g}$, the interaction can be shown to be approximately quadratic in the separation of the cores while for a larger separation, minimization of the LD free energy for a pair of layers leads to [8]

$$-|r_g \nabla \Phi|^2 + \sin\Phi = 0, \tag{3}$$

where $\Phi(x) \equiv \phi_{z+1}(x) - \phi_z(x)$. A more elaborate treatment gives a sine-Bessel-type equation [16] similar to Eq. (3) which has a nontrivial sine-Gordon kink solution leading to a "string" of vortex with the core running between the planes providing the necessary phase healing by 2π over a length scale given by r_g. For separation of the vortices beyond $2r_g$, an interplanar core will start to form with energy proportional to the distance. Thus, the interplanar Josephson coupling between two-dimensional vortices may be written in the following way:

$$\frac{a\phi_0^2}{8\pi^3\lambda^2}[1+\ln(\lambda/a)]\left(\frac{|R_i^{z,z+1}|}{r_g}-2\right), \text{ for } |R_i^{z,z+1}|>2r_g,$$
$$\frac{a\phi_0^2}{8\pi^3\lambda^2}[1+\ln(\lambda/a)]\left(\frac{|R_i^{z,z+1}|^2}{4r_g^2}-1\right), \text{ otherwise}, \tag{4}$$

where $R_i^{z,z+1}=|R_{iz}-R_{i,z+1}|$. For the in-plane interaction, a logarithmic potential is appropriate for the extreme limit of 2D planar vortices [17] while a $K_0(r/\lambda)$ potential is more suited for a 3D flux-line system [1]. For our system of finite size, we use the latter form and will justify its use in the discussion:

$$\delta F_{\text{in-plane}}(R_{i,z}-R_{j,z}) = \frac{\phi_0^2 d}{8\pi^2\lambda^2} K_0\left(\frac{|R_{i,z}-R_{j,z}|}{\lambda}\right). \tag{5}$$

Thus we approximate the full 3D interaction [18] with an effective 2D interaction restricted to the same plane and the short-ranged Josephson interlayer coupling.

In performing the Monte Carlo simulation, we followed the usual Metropolis algorithm on a system of 64 (or 16) flux lines confined to a 256 by 222 by 16 (or 32) grid space. Each flux line (indices i,j) may be viewed as a collection of beads connected by a flexible string, with each bead confined to move in a plane (index z). In a single Monte Carlo step, each bead makes a trial movement by a unit grid. We used the boundary conditions periodic in the x-y plane and free in the z direction. Periodic boundary conditions with a long-range potential also necessitate a proper treatment of the image potential, whose effect we incorporate through the Ewald-sum technique [19]. Throughout the simulation, the areal density of the system is fixed at a value determined by a selection of the length scale corresponding to a grid unit. For example, the choice of $\Delta x = a\lambda$, $\lambda = 2000$ Å, gives a magnetic field intensity of

$$B = n\phi_0 = \frac{(2.07\times10^{-7}\,\text{G cm}^2)\times 2}{(3a_0^2)^{1/2}\,\text{cm}^2} = \frac{0.145}{a^2}\,\text{G}$$

for vortices apart from the neighbors by 64 grid units. We studied a model with parameters similar to the $Bi_2Sr_2Ca_1Cu_2O_8$ system for which there are interesting experimental results available [20]. The other length-related parameter, $r_g = \xi_{ab}/\sqrt{g}$, is fixed by the choice of values for ξ and g. Taking $\kappa = 100$ and $\sqrt{g} = \frac{1}{50}$ as is appropriate for $Bi_2Sr_2Ca_1Cu_2O_8$ gives $r_g/\Delta x = 0.5/a$. Therefore, we vary the effective density of the flux lines by varying the length-scaling factor a while keeping the total number of the flux lines and the number of grid cells in the simulation fixed. The total number of vortices is explicitly conserved throughout the simulation and no creation of additional vortex pairs was allowed. Thus, it is not the Gibbs free energy, $\mathcal{G}_{\text{LD}}$ but $\mathcal{F}_{\text{LD}}$ that is minimized in our simulation and the phase diagram (Fig. 1)

represents $B(H)$ vs T rather than H vs T as is usual in experiments. The energy is scaled with $d\phi_0^2/8\pi^2\lambda^2 \equiv T_0$, where $\lambda^2 \approx \lambda_0^2/(1-T/T_c)$ was used. Using the value of 1.2×10^6 Å for $\lambda(0)^2/d$, we have $T_0 \approx 1000$ K placing our results in a reasonable range in the phase diagram. While slowly warming up the system [21], we measured the average of each component of the internal energy and energy fluctuations. The mean-square deviation of each particle position from its equilibrium position

$$(\delta R_{\text{in-plane}} \equiv \langle |R_{i,z} - R_{i,z}^{\text{ave}}|^2 \rangle^{1/2})$$

was measured to evaluate the Lindemann number for melting [22]. Another important quantity, especially for a system with many layers, is the "end-to-end" distance fluctuation

$$\delta R_{\text{end-to-end}} \equiv \langle |R_{i,z=1} - R_{i,z=Nz}|^2 \rangle^{1/2}.$$

The collective structure of the vortices was measured by the three-dimensional density-density correlation function and its Fourier transform variants along with the hexatic order parameter

$$\psi_6 \propto \left\langle \sum_{i=1}^{N} \frac{1}{z_i} \sum_{j=1}^{z_i} e^{i6\theta_{ij}(r_i)} \right\rangle,$$

where θ_{ij} is the bond angle between the neighbors (i and j) and z_i is the coordination number for vortex i. The pair correlation functions for the two types of order were also measured. The procedure was repeated with and without flux-line cutting.

To evaluate the reliability of the whole procedure, we ran the program on a well-known problem with an analytic solution [23]. We get excellent agreement between the simulation and the exact solution [24].

In Fig. 1, we show the bird's-eye view of our result in the form of a phase diagram. The temperature and the length scales were chosen for the $Bi_2Sr_2Ca_1Cu_2O_8$ system and no cutting of the vortices was allowed. The system is melted over most of the phase diagram, which spans five decades in density. We identified two phase-transition curves from our simulation. The lower temperature curve was determined by observing the disappearance of the in-plane translational order monitored by the peak of $S(\mathbf{q}=\mathbf{G}_1)$ which is the in-plane Fourier transform of the density-density correlation function at the first Bragg point. It has a very sharp peak in the solid phase but it decays and saturates in the liquid phase. We identify the point where the saturation is reached at T_m. This point also coincides with that at which the quantities $\delta R_{\text{in-plane}}(T)$ and $\delta R_{\text{end-to-end}}(T)$ show sharp changes in slope. The second curve is obtained from a similar analysis of the hexatic order parameter ψ_6. Details of the analysis will be given elsewhere. The melting seems to occur through two steps similar to what occurs in two-dimensional melting. We took a thorough look at the equilibrium configurations and found that the low-temperature and high-field regime exhibits in-plane order but the two-dimensional lattice planes wiggle as a whole. Beyond the $B=500$ kG limit in the figure, the simulation yields virtually independent-layer crystals asymptotically approaching the 2D limit. Following Huberman and Doniach [2], an upper limit for the melting temperature of an individual layer can be set to be $k_B T_m \leq (1/8\pi\sqrt{3})d\phi_0^2/16\pi^2\lambda^2$ which translates to $k_B T_m \leq 11.5$ K in our case. Given the fact that the renormalization of the interaction pulls that limit down [3] to 5–9 K, our result is in good agreement with the theoretical bounds. In the low-field regime, the interlayer coupling is relatively stronger than the in-plane correlations and the system displays straighter flux lines, forming a very fragile lattice. In the very-low-field limit, the melting temperature shifts downward drastically giving rise to a reentrant behavior as shown in the inset of Fig. 1. This behavior is expected since the vortices are so far apart from each other ($\lambda \gg a_0$) that the in-plane interaction is in the exponential limit. Since the flux lines are straight in the very-low-field regime ($|R_{i,z} - R_{i,z+1}| < \lambda \ll a_0$), we believe that it is more appropriate to use the K_0 potential to take better account of the vortices being closer to the 3D objects in the dilute regime. In that limit, the shielding from different layers should be more effective so that the in-plane interaction can no longer be considered localized in each layer.

The Lindemann constant (Fig. 2) as determined from the simulation ($\delta R_{\text{in-plane}}/a_0$) gives a reasonable value of about 0.2 but deviates in both the large-field and the low-field limits. Since we have two different types of interaction in the system which scale differently with length (i.e., by changing density), it is reasonable to expect such a behavior. It may also suggest that the nature of the melting changes as one goes from the 2D-like high-density (high-field) limit to the 3D-like low-density limit. The calculation in the continuum-elastic theory had used a somewhat larger value of 0.4 (dashed curve in Fig. 1) [22].

We finally discuss the effect of reconnection. Within

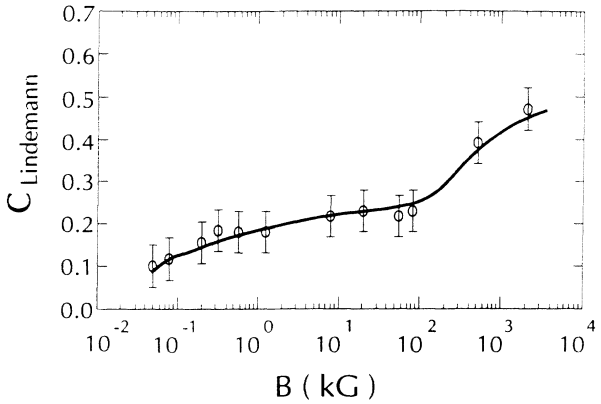

FIG. 2. The Lindemann criterion number [$\equiv(\delta R_{\text{in-plane}}/a_0)$] as a function of density (field intensity) was determined based on the lower-temperature melting curve of Fig. 1.

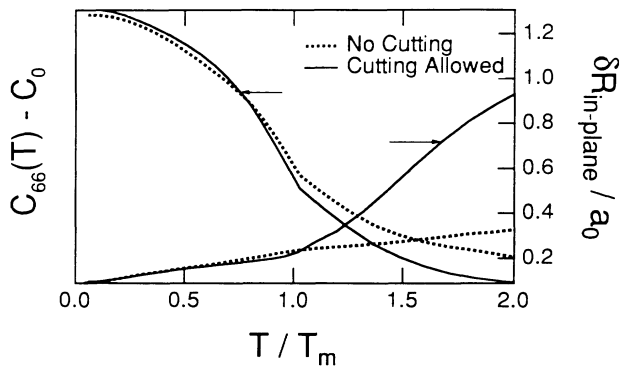

FIG. 3. Effect of allowing cutting and reconnection for $B = 20$ kG. In-plane shear modulus, c_{66} was calculated from ten equilibrium configurations for each temperature using the formula derived in Ref. [25]. The reference value c_0 was taken to be c_{66} evaluated at $2 \times T_m$ with cutting allowed. The right-hand side shows $\delta R_{\text{in-plane}}(T)/a_0$ which measures the in-plane fluctuation of each vortex from equilibrium position.

the coupled-planes model, vortices may switch connections to lower the elastic energy when they cross each other. We ran the same set of simulations in which cutting and reconnection were allowed. We take the energy barrier for the process in the following way. A pair of flux lines is given a probability for cutting when the lines are found in such a configuration that switching identities at and below a specific segment could decrease the energy. The probability is given by the Boltzman factor of the energy change. The energy barrier for cutting, then, is given by the potential field set by all the other vortices which the segments should have overcome to approach each other. We observe that the specific heat begins to rise at a slightly lower temperature but the order parameters do not show significant changes. However, the in-plane shear modulus [25] and the mean-square deviation from equilibrium position (Fig. 3) show sizable difference once flux cutting starts to occur. This will drastically change the entanglement effect and affect the viscous behavior [26].

One of the authors (S.R.) thanks Carlos A. R. Sá De Melo for the helpful and stimulating discussions. This work was supported by NSF Grants No. DMR-89-19803 (S.D.) and No. DMR-86-57658 (A.K.), by AFOSR Grant No. F49620-89-C-0001 (A.K.), and by the Israel-U.S. Binational Science Foundation (G.D.).

[1] D. R. Nelson, Phys. Rev. Lett. **60**, 1973 (1988); D. R. Nelson and H. S. Seung, Phys. Rev. B **39**, 9153 (1989).
[2] B. A. Huberman and S. Doniach, Phys. Rev. Lett. **43**, 950 (1979).
[3] D. S. Fisher, Phys. Rev. B **22**, 1190 (1980).
[4] D. R. Nelson and B. I. Halperin, Phys. Rev. B **19**, 2457 (1979); J. M. Kosterlitz and D. J. Thouless, J. Phys. C **6**, 1181 (1973).
[5] W. R. White, A. Kapitulnik, and M. R. Beasley, Phys. Rev. Lett. **66**, 2826 (1991).
[6] D. S. Fisher, M. P. A. Fisher, and D. A. Huse, Phys. Rev. B **43**, 130 (1991).
[7] M. V. Feigel'man, V. B. Geshkenbein, and A. I. Larkin, Physica (Amsterdam) **167C**, 177 (1990).
[8] S. Doniach, in *High Temperature Superconductivity, Proceedings*, edited by K. S. Bedell *et al.* (Addison-Wesley, Redwood City, 1989), p. 406.
[9] G. Deutscher and Kapitulnik, Physica (Amsterdam) **168A**, 338 (1990).
[10] L. Xing and Z. Tešanović, Phys. Rev. Lett. **65**, 794 (1990).
[11] Y.-H. Li and S. Teitel, Phys. Rev. Lett. **66**, 3301 (1991).
[12] W. E. Lawrence and S. Doniach, in *Proceedings of LT 12, Kyoto, 1970*, edited by E. Kanda (Keigaku, Tokyo, 1971), p. 361.
[13] See Eq. (41) of J. R. Clem, Phys. Rev. B **43**, 7837 (1991).
[14] In addition to Ref. [13], see also A. Buzdin and D. Feinberg, J. Phys. (Paris) **51**, 1971 (1990); S. N. Artemenko and A. N. Kruglov, Phys. Lett. A **143**, 485 (1990); L. N. Bulaevskii, S. V. Meshkov, and D. Feinberg, Phys. Rev. B **43**, 3728 (1991).
[15] The term $-(1/4\pi)\int \mathbf{H}_{\text{ext}} \cdot \mathbf{B}(r)\, d^3x$ can be shown to contribute zero in the thermodynamic limit under the condition of the fixed number of vortices through top and bottom of the sample as a result of London shielding.
[16] J. P. Carton, J. Phys. I (France) **1**, 113 (1991).
[17] J. Pearl, J. Appl. Phys. **37**, 4139 (1966).
[18] E. H. Brandt, Phys. Rev. Lett. **63**, 1106 (1989). We have neglected string-string interactions which lead to the Biot-Savart-like form in the continuum limit. Following our results, this neglect should not be important at either low or high fields. According to the above reference, a rigorous treatment of the full 3D interaction may further reduce the melting temperature.
[19] M. Inui, S. Doniach, and M. Gabay, Phys. Rev. B **38**, 6631 (1988).
[20] For example, C. A. Murray, P. L. Gammel, D. J. Bishop, D. M. Mitzi, and A. Kapitulnik, Phys. Rev. Lett. **64**, 2312 (1990).
[21] From a run of "simulated annealing" type, we find the triangular lattice to have lower energy than the square lattice for our choice of the interaction and material parameters. Thus, we start with a triangular lattice as the initial configuration at low temperature.
[22] A. Houghton, R. A. Pelcovits, and A. Sudbo, Phys. Rev. B **40**, 6763 (1989).
[23] M. L. Mehta, *Random Matrices* (Academic, San Diego, 1991), 2nd ed., Chap. 4.
[24] In this model, $H = \frac{1}{2}\sum_i x_i^2 - \sum_{i<j} \ln|x_i - x_j|$ in 1D.
[25] D. R. Squire, A. C. Holt, and W. G. Hoover, Physica (Utrecht) **42**, 388 (1969).
[26] M. C. Marchetti and D. R. Nelson, Phys. Rev. B **42**, 9938 (1990).